PAPER

Biocatalytic cascade combining an engineered pyranose 2-oxidase and transaminases for the synthesis of amino sugars

Litavadee Chuaboon,[ab] Surawit Visitsatthawong,[c] Orawan Sookbampen,[b] Siripakorn Suthin,[b] Moritz Voss,[d] Thanyaporn Wongnate, [c] Matthias Höhne,[e] Uwe T. Bornscheuer [*d] and Pimchai Chaiyen [*c]

This work reports cascade reactions using a pyranose 2-oxidase and transaminases for synthesizing the rare amino sugars mannosamine, glucosamine, and galactosamine. Transaminases were engineered to accept unnatural 2-keto-sugars, providing up to 68% galactosamine yield. The mechanisms of C2-amination by these transaminases were also investigated. These transaminase variants have potential applications in high-value amino sugar synthesis.

1 Introduction

C2 chiral amino sugars are important synthons in various fields. For instance, glucosamine is used as a commercial supplement for treating bone and joint disorders.[1] Amino sugars can also be used as building blocks for synthesizing medically relevant carbohydrate materials.[2–4] Galactosamine, allosamine and glucosamine are also useful for the synthesis of chiral ligands valuable for many asymmetric catalytic reactions.[5,6] The use of classical organic synthesis approaches to synthesize amino sugars is cumbersome due to the inherent stereochemistry of carbohydrates and the need for protecting group chemistry.[7] In addition, chemical methods for synthesizing glucosamine, galactosamine and mannosamine involve protecting and deprotecting anomeric and other groups in sugars.[8,9] Some of the methods involve up to four steps including C2 protection by an azide, and require a rare sugar and thiomannoside as starting materials. The process involves displacing triflates at the C2 position with azide, yielding glucosamine building blocks in 70% yields after two days.[10] Although the biosynthesis of amino sugars can be carried out in microorganisms, it requires the use of expensive starting materials such as sugar phosphates or sugar nucleotides.[11] Therefore, a new, alternative method is needed to establish environmentally friendly industrial processes that can produce amino sugars without complicated protection and deprotection steps and using inexpensive starting precursors.

Asymmetric synthesis using transaminases (TA) is attractive as a biocatalytic tool for chiral amine synthesis[12,13] as these pyridoxal-5′-phosphate-(PLP) dependent enzymes catalyze stereoselective amino group transfer using widely available amino donors such as alanine or isopropylamine. Two transaminases from *Mycobacterium vanbaalenii* TA (*Mv*-TA) and from *Rhodobacter sphaeroides* TA (*Rh*-TA) can accept a variety of sugars derived from biomass to produce aminopolyols, which are ingredients in cosmetic applications.[14] The direct amination of aldoses at C1 of various monosaccharides catalyzed by the transaminase ATA256-TA could create valuable chiral ω-amino alcohols.[15] A two-step cascade reaction of galactose oxidase with *Cvi*-TA was used to add an amino group at C6 of galactose to generate a novel amino sugar.[16] Currently, there are no reports of effective biocatalytic processes for C2 amino sugar production because this would first require highly specific oxidation at the C2 hydroxy group position of a monosaccharide.

The pyranose 2-oxidase (P2O) from *Trametes multicolor* is a flavoenzyme which can catalyze the regio-specific oxidation of common sugars at the C2-position to generate 2-keto sugars.[17] Its reaction mechanism and applications have been extensively investigated.[18–24] Sugar oxidation by P2O is a green process because the by-product of the reaction (H$_2$O$_2$) can be easily removed by adding catalase to generate oxygen and water. Therefore, we proposed to use an engineered P2O in combination with a TA to produce chiral amino sugars in this enzymatic cascade (Fig. 1).

Herein, we report a cascade reaction utilizing a P2O and TAs to synthesize the valuable C2 chiral amino sugars D-mannosamine and D-galactosamine from the common and low-cost

[a]School of Pharmacy, Walailak University, Nakhon Si Thammarat, 80160, Thailand

[b]Biomass and Oil Palm Center of Excellence, Walailak University, Nakhon Si Thammarat, 80160, Thailand

[c]School of Biomolecular Science and Engineering, Vidyasirimedhi Institute of Science and Technology (VISTEC), Wangchan Valley, Rayong 21210, Thailand. E-mail: pimchai.chaiyen@vistec.ac.th

[d]Institute of Biochemistry, Department of Biotechnology and Enzyme Catalysis, Greifswald University, Felix-Hausdorff-Strasse 4, 17487 Greifswald, Germany. E-mail: uwe.bornscheuer@uni-greifswald.de

[e]Technical University of Berlin, Institute of Chemistry, Straße des 17. Juni 135, Sekr. L1, 10623 Berlin, Germany
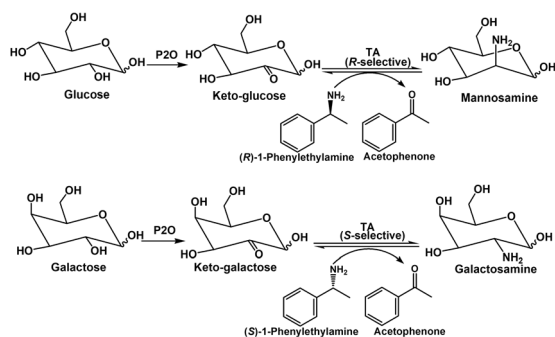
Fig. 1 Stereoselective synthesis of C2 chiral amino sugars using cascade reactions utilizing variants of a P2O and a transaminase.

sugars, D-glucose and D-galactose. As these 2-keto-sugars are not native transaminase substrates, enzyme engineering was needed to create highly active (S)- and (R)-selective TAs. We used molecular docking of keto-sugars and tunnel analysis of

transaminases to create enzymes with the desired equatorial/axial-selectivity.

2 Results and discussion

2.1 Screening (R)- and (S)-selective transaminases for mannosamine and galactosamine synthesis

In this study, C170A and T169G variants of P2O were chosen as biocatalysts to generate 2-keto-sugars because they have shown potential in generating 2-keto-glucose and 2-keto-galactose.[22] For the transaminase-catalyzed reaction, we used the (R)-selective TA from *Aspergillus fumigatus Af293* (*Asp*) and the (S)-selective TA from *Chromobacterium violaceum* (*Cvi*) as starting enzymes to investigate their ability for stereoselective C2 amino sugar synthesis.[25,26] It is important to note that a broad pH screening of both engineered P2O and transaminase was conducted to identify the best condition to drive the overall reaction forward. Reactions of the purified TAs were screened using the *o*-xylylene diamine assay[27] at different pH values. Dark-colored precipitates of isoindoles indicate the desired transaminase
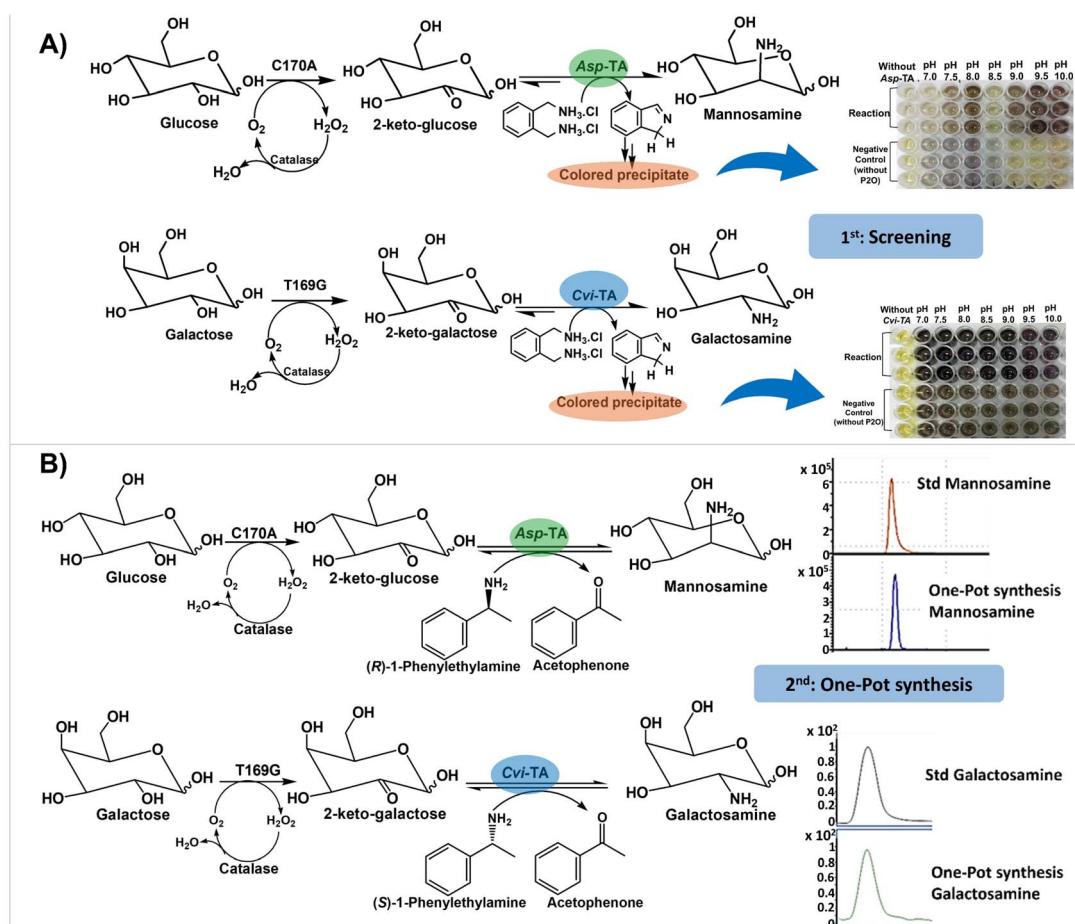

Fig. 2 Screening of transaminases. (A) High-throughput screening of transaminases using the *o*-xylylene diamine assay.[27] Reactions were performed in triplicate. (B) One-pot synthesis of mannosamine (upper panel) and galactosamine (lower panel) from reactions catalyzed by a P2O and a transaminase. The upper panel reaction shows the formation of mannosamine while the lower panel shows formation of galactosamine. The amino sugars were identified using LC–MS/MS analysis compared to the mannosamine and galactosamine standards. Reactions contained 5 mM sugar, 10 mM amine donor, 1 μM of P2O variants, and 7 mg mL^{-1} of transaminase variants. Reactions were run at 1 mL scale in 50 mM HEPES buffer (pH 7) at 30 °C for 12 hours.

activity. *Asp*-TA showed this dark precipitation at pH 8, 9, 9.5, and 10, whereas *Cvi*-TA was active from pH 7–10 (Fig. 2A). We also performed screening with other (*S*)-selective transaminases (3HMU from *Ruegeria pomeroyi*[28] and TA10 from *Burkholderia multivorans*).[29] However, the negative control reaction of the diamine assay using 3HMU and TA10 containing sugar substrate and transaminase (without P2O) showed more dark precipitate when compared to the negative control reaction of *Cvi*-TA (Fig. S2, ESI). We assumed that 3HMU and TA10 might react with the sugar substrate in its open ring form at the C1 aldehyde position, resulting in the formation of an amino alcohol. This agrees with the previous findings reported by Cairns *et al.*[15] regarding the direct amination of aldose sugars by 3HMU. Thus, we selected *Cvi*-TA for galactosamine synthesis as it had the lowest background activity.

We further confirmed the abilities of *Asp*-TA and *Cvi*-TA in mannosamine and galactosamine synthesis using one-pot reactions together with P2O. LC-MS/MS analysis showed that both transaminases converted 2-keto-glucose and 2-keto-galactose to yield mannosamine (10% conversion) and galactosamine (15% conversion), respectively (Fig. 2B).

2.2 Elucidating stereospecificity of *Cvi*-TA and *Asp*-TA to keto-sugar by molecular docking

To increase the yields of the mannosamine and galactosamine syntheses, we engineered *Asp*-TA and *Cvi*-TA using semi-rational methods. We first identified residues important for binding 2-keto-sugars and then analyzed the formation of the intermediate 2-keto-sugars-PMP complex (the planar quinonoid) using molecular docking and mechanistic analyses. Based on the established TA mechanism,[30] we assumed that the second half-reaction (Fig. 3A) in which the amino group is transferred from the enzyme-bound PMP to the 2-keto-sugar (step 1) leads to the formation of a planar quinonoid (step 6). Subsequently, the catalytic lysine protonates this quinonoid to yield a chiral amino sugar and this step is crucial for controlling the stereoselectivity of the transamination. We thus used CAVER analyst and molecular docking to identify tunnels and to study the binding mode of 2-keto-glucose in step 1 to propose the structure of the planar quinonoid for step 6 (Fig. 3B).[31]

We identified that *Cvi*-TA and *Asp*-TA have different geometries in the formation of the planar quinonoid (step 6), which leads to different orientations for transamination (equatorial or axial). Analysis of tunnels and molecular docking in *Asp*-TA showed that the catalytic lysine (K179) can only donate a proton to the top face of the pro-chiral imine of the planar quinonoid (4.0 Å). This proton is then donated to the equatorial position, resulting in formation of the axial amino sugar in *Asp*-TA. In contrast, in *Cvi*-TA, the catalytic lysine (K288) can only donate a proton to the bottom face (axial position) of the prochiral imine (2.6 Å), resulting in formation of the equatorial amino sugar in *Cvi*-TA (Fig. S3 and S4, ESI).

2.3 Enzyme engineering by site-directed mutagenesis for enhancing mannosamine and galactosamine synthesis

To further enhance the efficiency of the amino sugar synthesis, we engineered residues located around the binding site of the 2-keto sugar and the planar quinonoid (Tables S1 and S2, ESI). Briefly, we selected the following residues based on their proximity to specific groups of the 2-keto sugar substrate and the planar quinonoid intermediate: (i) residues located near the C1 and C2 hydroxyl groups of the 2-keto sugar substrate and the phosphate group of the planar quinonoid including Y58 and T273, (ii) residues located near the C3, C4, and C6 hydroxyl groups of the 2-keto sugar substrate and the hydroxyl group of the planar quinonoid including R126 and R416, (iii) residues located near the tunnel of the 2-keto sugar substrate and the planar quinonoid including F113, W183, and F88. The results showed that the *Asp*-TA T273A variant gave the highest mannosamine production, with a 2.1-fold increased yield compared
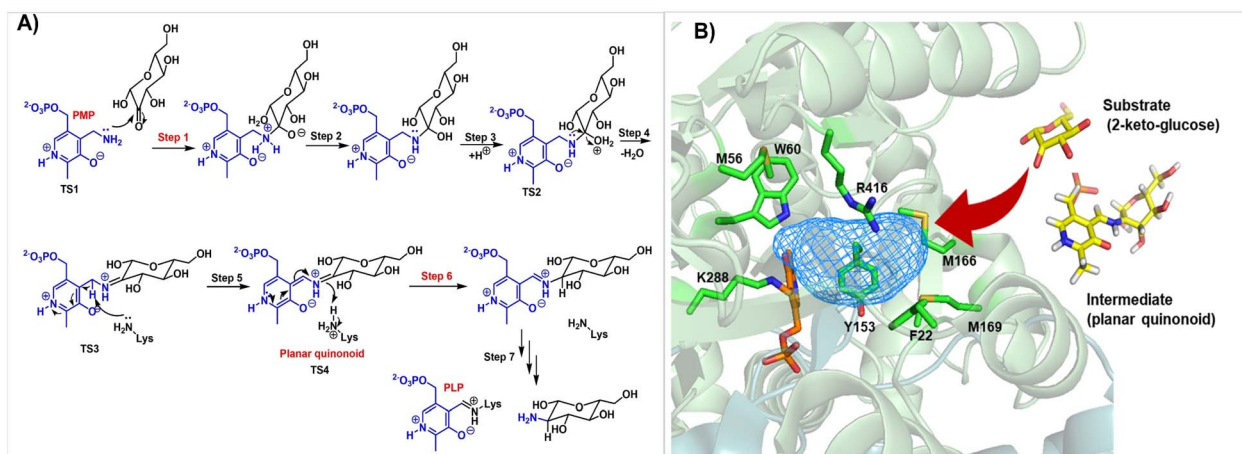

Fig. 3 (A) Proposed mechanism of the second half-reaction of keto-sugar transamination catalyzed by the transaminase. TS1: pyridoxamine-5′-phosphate (PMP) attacks the keto-sugar (step 1). TS2: PMP eliminates water from the keto-sugar (step 4). TS3: Lys abstracts a proton from PMP forming the planar quinonoid (step 5). TS4: Lys donates a proton to the keto-sugar (step 6). (B) Tunnel analysis and molecular docking of the keto-sugar to the PMP-bound enzyme and the planar quinonoid intermediate to the apo enzyme were used to identify target residues in enzyme engineering.
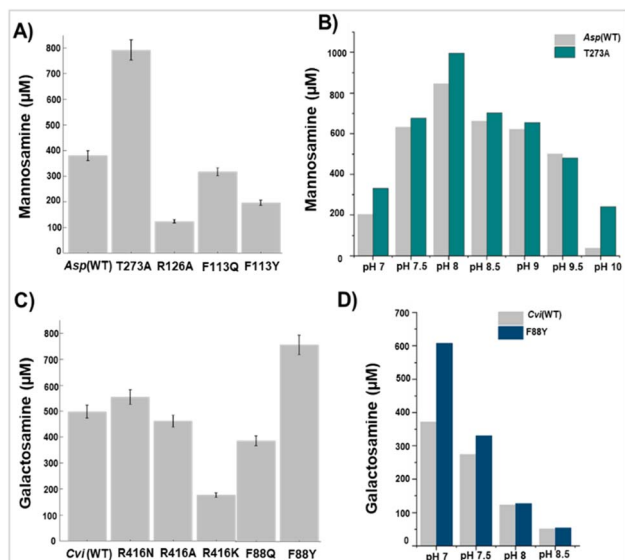
Fig. 4 Screening of variants of *Asp*-TA and *Cvi*-TA for mannosamine (A) and galactosamine (C) synthesis. (B) pH optimization for the reaction of T273A (green bar) variant compared to that of wild-type *Asp*-TA (gray bar). (D) pH optimization for the reaction of the F88Y (blue bar) variant compared to that of wild-type *Cvi*-TA (gray bar).

to the wild-type *Asp*-TA (Fig. 4A). The optimal conditions for bioconversion were at pH 8 (Fig. 4B), and the ratio of glucose : (*R*)-PEA at 1 : 4 (Fig. S5, ESI). For galactosamine synthesis, the F88Y variant of *Cvi*-TA gave the highest galactosamine formation with a 1.5-fold increase compared to the wild-type enzyme (Fig. 4C). Optimization of the ratio of galactose : (*S*)-PEA at 1 : 1 and pH 7 gave the highest galactosamine formation (Fig. 4D). However, when the concentration of (*S*)-PEA exceeded 5 mM, galactosamine production decreased greatly possibly due to substrate inhibition. In contrast, mannosamine synthesis catalyzed by *Asp*-TAs showed no substrate inhibition (Fig. S6, ESI).

2.4 Mannosamine and galactosamine synthesis through a one-pot reaction using engineered P2O and transaminase

T273A, the best variant from the screening reaction, was used to synthesize mannosamine and to explore intermediate formation during multiple turnover reactions of P2O (C170A) and *Asp*-TA (T273A). This cascade reaction resulted in 28% conversion to mannosamine (Table 1). The intermediate 2-keto-glucose showed a peak early in the process and then decreased as it was further converted into mannosamine (Fig. S7 and S8, ESI). We found a peak area at 193 *m/z* which increased during the reaction progress (Fig. S9, ESI). This peak was likely due to the second oxidation by P2O followed by the hydrolysis in the last step to generate 2-keto gluconic acid (193 *m/z*). These results agree with our previous findings that sugar acids can be generated from P2O reactions.[24]

The synthesis of galactosamine, utilizing the best variant F88Y of *Cvi*-TA and T169G (P2O), achieved 34% conversion (Table 1). For D-galactosamine synthesis, we detected formation

Table 1 C2 chiral amino sugars synthesis by the enzyme cascade utilizing P2O and transaminase variants

Entry	Biocatalysts P2O : TA	pH	Ratio sugar : PEA	Conversion (%)
1	C170A : *Asp* (WT)	8	1 : 4	14[a]
2	C170A : T273A	8	1 : 4	28[a]
3	T169G : *Cvi* (WT)	7	1 : 1	18[b]
4	T169G : F88Y	7	1 : 1	34[b]
5	C170A : F88Y	7	1 : 1	25[c]

[a]Mannosamine   [b]Galactosamine   [c]Glucosamine

of 2-keto galactose as an intermediate and 2-keto galactonic acid as an alternative product (Fig. S7 and S8, ESI), similar to those observed during the synthesis of mannosamine. When we performed glucosamine synthesis to observe patterns of amino sugar and sugar acid formation using cascade biocatalysis using the F88Y and C170A variants, we found that glucosamine was formed (25% conversion) (Table 1) as well as 2-ketogluconic acid (Fig. S9, ESI). This demonstrates that a one-pot conversion of common sugars to amino sugars employing P2O and TA is possible with 25–34% analytical yield; however, formation of the alternative sugar acid product was also possible.

Docking analysis showed that the T273A variant would allow an appropriate keto-sugar and planar quinonoid binding because of a decreased steric effect as this residue is located near the C2–OH of the keto-sugar (3.5 Å) and the phosphate group of the planar quinonoid (2.9 Å) in *Asp*-TA (Table S1). The F88Y variant may alter sugar binding because the F88 residue is part of tunnels for keto-sugar access to the active site, possibly assisting the planar quinonoid formation (Fig. S4, ESI). According to our *in silico* model, the hydroxyl group of the tyrosine 88 side chain can indeed form hydrogen bonds with sugar molecules. This interaction is crucial for high-affinity binding as the hydrogen bonds would facilitate precise sugar binding within the binding tunnel.

For improving amino sugar synthesis, a two-step reaction setup and the addition of DMSO co-solvent to increase substrate solubility[32] was utilized to decrease sugar acid formation. The formation of 2-keto galactose (an intermediate) and sugar acid (a by-product) was monitored using LC-MS/MS (Fig. S7). These data allowed us to determine that adding the transaminase after 4 hours was the optimal time to initiate the second reaction step. We chose this time point because it yielded the highest production of 2-keto galactose and the lowest production of sugar acid. Galactosamine yield could be improved in the two-step reaction using 10% DMSO, achieving 68% product formation (Table 2). This condition also reduced the sugar acid by-product formation to 23% (Table 2). However, one-pot reactions could not be used to improve the yield, possibly due to enzyme denaturation in the presence of DMSO.

Table 2 Effects of the reaction set-up and DMSO concentration on galactosamine and sugar acid (by-product) formation utilizing the cascade reaction of P2O-T169G and the *Cvi*-TA-F88Y variants

Reactions	Conversion into galactosamine (%)	% Relative of sugar acid (by-product)[a]
One-pot reaction 2.5% DMSO	32	100
One-pot reaction 10% DMSO	48	65
Two-step reaction 10% DMSO	68	23

[a] % Relative amount of sugar acid was calculated based on the peak area of sugar acid by LC-MS detection. The highest peak area was considered as 100%.

The high polarity and hydrophilicity of sugars make it challenging to separate amino sugar products using conventional extraction methods. To overcome this, we added the protecting group fluorenylmethoxycarbonyl (Fmoc) to galactosamine, creating 9-fluorenylmethoxycarbonyl-galactosamine (Fmoc-galactosamine). This product was then purified using a preparative HPLC (Fig. S10). The purity of Fmoc-galactosamine was confirmed using high resolution mass spectrometry (MS) (Fig. S11). Galactosamine was selected for characterization because it could be obtained with the highest conversion.

3 Conclusions

In conclusion, P2O and TA variants were used in combination as valuable biocatalysts for the synthesis of C2 chiral amino sugars. Our work here presents a novel strategy for the synthesis of mannosamine and galactosamine using a cascade reaction. The T273A variant of *Asp*-TA prefers axial amination and is suitable for mannosamine production whereas the F88Y variant of *Cvi*-TA prefers equatorial amination and can be used for galactosamine synthesis. Molecular docking explained the differences in stereoselectivity of *Cvi*-TA and *Asp*-TA. The two-step sequential reaction catalyzed by the transaminase variants T169G and F88Y could be used to enhance galactosamine synthesis and to reduce sugar acid formation. This study provides a platform for further investigations into the scalable biosynthesis of structurally diverse amino sugars, which are valuable for glycoscience and medicinal chemistry. Our study only presents a foundational enzymatic route for amino sugar synthesis. To achieve industrial feasibility, future efforts must focus on optimizing the biocatalytic process and developing advanced downstream processing technologies to overcome current challenges.

4 Experimental procedures

4.1 Preparation and purification of enzymes

For P2O preparation, the plasmids containing genes encoding the P2O variants from (UniProtKB accession: Q7ZA32)[33] (C170A for glucose as a substrate and T169G for galactose as a substrate) were transformed into *E. coli* BL21 (DE3) using the heat-shock transformation protocol. A single colony corresponding to each variant was selected from an LB agar plate (supplemented with 50 μg per mL ampicillin), inoculated, and grown in auto-induction medium (100 mL ZYM-5052 auto-induction medium, 50 μg per mL ampicillin). The culture was incubated overnight in an orbital shaker at 37 °C, 200 rpm. An overnight culture (5 mL) was inoculated into 6 (Erlenmeyer flask) × 650 mL of ZYP-5052 auto-induction medium containing 50 μg per mL ampicillin. The large-scale cell culture was incubated in an orbital shaker at 37 °C until the absorbance at 600 nm reached 1 (~3 h). The culture was allowed to grow at 16 °C overnight and then harvested by centrifugation at 7670 × *g* for 10 min at 4 °C. Cells were stored at −80 °C until used. The yield of the cell paste was ~50 g per L culture. The cell pellet was lysed by ultrasonication. P2O variants from crude lysate were purified using ammonium sulphate precipitation and ion-exchange DEAE chromatography.[17]

The plasmids containing genes encoding the transaminases including (i) pET28a-*Cvi*-TA[26] (UniProtKB accession: Q7NWG4), pET22b-3HMU-TA[28] (UniProtKB accession: Q5LMU1), pET28a-TA10 (ref. 29) (GenBank accession: MT828903) for (*S*)-selective transaminases and (ii) pET22b-*Asp*-TA[25] (UniProtKB accession: Q4WH08) for (*R*)-selective transaminase were transformed into *E. coli* BL21 (DE3) using the heat-shock transformation protocol. The resulting transformant was grown on an LB agar plate at 37 °C containing 100 μg per mL ampicillin for *Asp*-TA and 3HMU-TA, 50 μg per mL kanamycin for *Cvi*-TA and TA-10. A fresh single colony of transformant was inoculated in LB medium with antibiotic at 37 °C, 150 rpm for 16 h. Terrific Broth medium (TB) and isopropyl β-ᴅ-1-thiogalactopyranoside (IPTG) were used to grow the cell culture and express transaminase at 20 °C. Expression of *Cvi*-TA, *Asp*-TA, 3HMU-TA was induced using 0.5 mM IPTG after OD600 reached 0.8. TA-10 was induced using 1 mM of IPTG after the OD600 reached 1.2. The cultures were shaken (160 rpm) for an additional 16 h. The cell paste of each transaminase was harvested by centrifugation (7670 × *g*, 10 min, 4 °C). The cell pellet of each transaminase was suspended in lysis buffer containing 50 mM HEPES pH 7.5, 300 mM NaCl, 10 mM imidazole, and 0.1 mM PLP. Cells were disrupted by ultrasonication while controlling the temperature at 15 °C on ice-bath. Cell debris was removed from the supernatant by centrifugation at 16 128 × *g* at 4 °C for 1 hour. The immobilized metal affinity chromatography (IMAC) containing nickel or cobalt was used to purify his-tagged-transaminases. Metal affinity chromatography was equilibrated with 10-fold column volumes with lysis buffer before loading the enzymes. After loading an enzyme solution, 10-fold column volumes of wash buffer containing 50 mM HEPES pH 7.5, 300 mM NaCl,

20 mM imidazole, and 0.1 mM PLP were passed through the column to remove other proteins. Elution of protein was done using the wash buffer with increasing imidazole to 300 mM. The yellow transaminase was collected and exchanged into 50 mM HEPES and 0.1 mM PLP pH 7.5 using PD10 column or SephadexTM G-25 (GE healthcare) column. The purified transaminases were stored at −20 °C containing 20% glycerol. Transaminases purities were analyzed by SDS-PAGE and the concentrations were determined by the bicinchoninic acid assay (BCA assay).

4.2 Screening of (*R*) and (*S*)-selective transaminases

A high-throughput screening (HTS) to identify the desired transaminase activities was performed using the *o*-xylylenediamine assay.[26] The enzyme reactions contained 10 mM sugars (glucose/galactose), 2 μM P2O variants (C170A for glucose and T169G for galactose), 10 μM transaminase, 10 mM *o*-xylylenediamine dihydrochloride with the volume adjusted to 200 μL by adding different buffer solutions (50 mM HEPES for pH 7.0–8.0 and 50 mM CHES for pH 8.5–10.0). The plates were incubated at 30 °C in a shaker incubator at 220 rpm overnight. When an amine group in *o*-xylylenediamine is converted to an aldehyde, the resulting aldehyde undergoes intramolecular cyclization with a second amine group to form an isoindole. This isoindole is highly reactive, leading to formation of a colored polymeric product as a dark precipitate. Formation of intensely colored solutions and significant quantities of dark precipitation thus indicate the candidate activities. For a positive control, 10 mM pyruvate was added instead of sugar. The enzyme reaction without adding any transaminase or P2O was used as a negative control.

To confirm formation of mannosamine and galactosamine in the reactions catalyzed by the (*R*)- and (*S*)-selective transaminases, reactions of each transaminase and P2O were carried out and then analyzed by LC-MS/MS. Reaction mixtures typically contained 5 mM sugar substrates, 10 μM P2O variant, 50 μM transaminase, 2% w/v catalase, 10 mM (*R,S*)-PEA (as amino donor) in 50 mM HEPES pH 7.5 containing 0.1 mM PLP. A clear solution after removing denatured protein by centrifugation and microcon ultrafiltration was analyzed using an Agilent 6490 triple quadrupole mass spectrometer with an electrospray ionization source (ESI) equipped with an ultra-performance liquid chromatography system (LC-MS/MS) (Agilent technology, USA). An Asahipak NH2P-50 2D column (150 mm, 5 μm, Shodex) was used for detection of amino sugars. A mobile phase with 20% v/v 10 mM ammonium acetate and 80% v/v acetonitrile at a flow rate of 0.3 mL min⁻¹ was used as an eluent. MS conditions in LC-MS/MS were set to MRM mode to detect mannosamine and galactosamine.

4.3 Tunnel analysis and computational molecular docking

4.3.1. Tunnel analysis by CAVER analyst. CAVER analyst 2.0 (ref. 31) was used to find tunnels in *Cvi*-TA and *Asp*-TA. For *Cvi*-TA, the crystal structure of the enzyme in complex with PLP (PDB: 4a6t) was used.[25] The position of NZ of LYS-288, a catalytic residue, of Chain A was chosen as a starting point. A minimum

probe radius used was 0.9 Å. For *Asp*-TA, the enzyme crystal structure in complex with PLP (PDB: 4chi) was used.[24] The position of NZ of LYS-179, a catalytic residue, of Chain A was chosen as a starting point. A minimum probe radius was 0.9 Å.

4.3.2. Molecular docking of 2-keto-glucose. The purpose of this step is to identify the binding mode of 2-keto-glucose in step 1 (Fig. 3A) and model the structure of 2-keto-sugars-PMP complex (the planar quinonoid) for step 6. The structure of 2-keto-glucose was modified from 3-deoxy-3-fluoro-beta-ᴅ-glucose (3FG) from the crystal structure of H167A P2O in complex with 3FG, PDB 3PL8.[34] First, the molecular structure in the gas phase was optimized to obtain a reasonable starting point. This process helps understand the geometry and electronic structure of the molecules without the influence of solvent or charge. The gas-phase optimization of 2-keto-glucose was done using B3LYP[35–37]/6-31G(d)[38–40] equipped in Gaussian16 program.[41] Then, the PDB files of 4A6T and 4CHI were used as *Cvi*-TA and *Asp*-TA structures for calculations, respectively. Ligand and protein were prepared by AutoDockTools.[42,43] PLP was not modified to PMP to maintain the original structure as the status of cofactor should not affect the binding mode of 2-keto-glucose. The center of the docking box was the red point on the tunnel. The docking box size was 25 × 25 × 25 Å. Arg-416 in Chain A of *Cvi*-TA and Arg-126 in Chain B of *Asp*-TA were chosen as flexible residues (its side chain can rotate during docking calculation) in docking because it has a high dynamic. To assign protonation states and optimize the hydrogen bond network of amino acids in proteins, we used PROPKA which is a fast empirical method that predicts the pK_a values of ionizable groups in proteins based on their 3D structure.[44] The protonation states of amino acids were selected based on PROPKA[45] and optimal hydrogen bond network. Crystallographic water molecules were removed prior to docking. Flexible docking was performed by AutoDock Vina.[46]

4.3.3. Molecular docking of the planar quinonoid. The purpose of this step was to identify the binding mode of the planar quinonoid (2-keto-sugars-PMP complex) in step 6 with the desired product stereochemistry (Fig. 3A). The structure of the planar quinonoid was modified based on the structure derived from pyridoxal-5′-phosphate (PLP) and 2-keto-glucose. The planar quinonoid was subjected to geometry optimization using the same method described in the previous section. In the ligand preparation step, the C–N bond of planar quinonoid was fixed to be non-rotatable due to its partial double bond character. The center of the docking box was C4a of PLP. PLP was removed from the crystal structure before planar quinonoid docking. Arg-416 in Chain A of *Cvi*-TA and Arg-126 in Chain B and Phe-113 in Chain A of *Asp*-TA were chosen as the flexible residues (its side chain can rotate) in docking because it has a high dynamic. Other parameters of docking are the same as described in the previous section.

4.4 Enzyme engineering by site-directed mutagenesis

Based on the tunnel analysis and computational molecular docking of the *Cvi*-TA and *Asp*-TA with 2-keto-glucose and planar quinonoid bound, residues surrounding the binding site

were identified (Tables S1 and S2). Variants of candidate residues were created using PCR with specific primers (Table S3). The PCR (50 μL) contained plasmids of TAs (2–10 ng), primers (0.5 μM), dNTPs (200 μM), and Phusion™ High–Fidelity DNA polymerase (0.02 U μL^{-1}). The resulting PCR products were digested by restriction endonuclease *Dpn* I for 30 minutes at 37 °C and heat inactivated at 80 °C for 20 minutes. The PCR products were transformed into competent cell *E. coli* XL1blue. Desired mutations were validated by DNA sequencing. Variants were expressed and purified with the same method described in Section 4.1.

4.5 Mannosamine and galactosamine synthesis through bioconversion using transaminase and P2O

To screen variants of transaminase and to optimize the reactions, a solution of P2O and each transaminase variant was mixed with different buffer solutions containing 0.1 mM PLP and 1 mg per mL catalase (50 mM HEPES for pH 7.0–8.0 and 50 mM CHES for pH 8.5–10.0) and different ratios of sugar : EA concentrations. The enzyme reactions contained 5 mM sugars (glucose/galactose), 1 μM of P2O variants (C170A for glucose and T169G for galactose), 7 mg per mL transaminase variants and adjusted volume to 200 μL. This one-pot reaction was allowed to proceed at 37 °C and shaken at 220 rpm for 12 h. To follow reaction progress and to observe side product formation, the reaction volume was adjusted to 10 mL. Samples were collected and quenched by adding acetonitrile at a ratio of 1.5 : 1 (v/v).

For the two-step sequential reaction, the oxidation of P2O was set up and 2-keto sugar formation was detected by LC-MS/MS. The P2O variant was removed using a membrane filtration process using a Microcon ultrafiltration unit (10 kDa cutoff). Then, the transaminase reaction was initiated by adding PEA, DMSO and transaminase variant for 12 h.

4.6 Analysis of production formation by LC-MS/MS mass spectrometry

All samples were analyzed by LC-MS/MS using an Agilent 6490 triple quadrupole mass spectrometer with an electrospray ionization source (ESI) equipped with an ultraperformance liquid chromatography system. The MS conditions in LC-MS/MS (Table S4) were set to MRM mode to monitor sugar substrates, amino sugar products and intermediate species. A preparative column Asahipak NH2P-50 10E (10.0 × 250 mm, 5μm) was used for separating sugar substrates, amino sugar products and intermediates. A mobile phase used was 20% of 10 mM ammonium acetate and 80% acetonitrile at a flow rate of 1 mL min^{-1} and the column temperature was set at 15 °C. Multiple turnover reactions of candidate transaminase variants described above for synthesizing mannosamine and galactosamine were analyzed for peak areas of substrate, product and intermediate at various time points during multiple turnover reactions. MS/MS data collection were done using qualitative/quantitative analysis by the MassHunter software (Agilent).

4.7 Synthesis of 9-fluorenylmethoxycarbonyl-galactosamine

The derivatization reaction was conducted in a 0.2 M borate buffer (pH 7.0) containing 129.35 mg L^{-1} of Fmoc-Cl and the reaction sample with 60–150 nmol of galactosamine hydrochloride (standard or from the biocatalytic reaction). The mixture was incubated at 25 °C for 30 minutes. After incubation, the reaction mixture was evaporated and freeze-dried. The freeze-dried sample was redissolved in a 50 : 50 solution of 2-propanol and acetonitrile, and then filtered through a 0.22 μm microporous membrane filter for HPLC-DAD analysis and purification.HPLC analysis was performed using a Fortis C18 column (5 μm, 150 mm × 4.6 mm). The HPLC-diode array detector (DAD) was set to a wavelength of 254 nm at 30 °C. The mobile phase consisted of water (A) and acetonitrile (B). A linear gradient was applied, increasing from 30 to 100% of mobile phase B over 12 min, followed by a 2-minute hold at 100% of mobile phase B. The flow rate was set at 1.0 mL min^{-1}, with a 1000 μL loop injection. The HPLC-DAD detector was used to monitor the individual constituents, and fractions of (Fmoc-galactosamine) were collected based on targeted peak detection. The final product's purity and identity were confirmed by mass spectrometry (MS).

Author contributions

LC: conceptualization, methodology, investigation, formal analysis, writing – original draft, funding acquisition. SV: methodology, investigation, formal analysis. OS: methodology, investigation. SS: methodology, investigation. MV: methodology, investigation. TW: writing – reviewing and editing. MH: writing – reviewing and editing. UB: conceptualization, investigation, visualization, writing – review & editing, project administration. PC: conceptualization, investigation, visualization, writing – review & editing, project administration. All authors approved the manuscript version to be published.

Conflicts of interest

There are no conflicts to declare.

Data availability

Supplementary information: the data supporting this article are available in the main manuscript and SI. See DOI: https://doi.org/10.1039/d5ra04556h.

Acknowledgements

Notes and references

1 D. O. Clegg, D. J. Reda, C. L. Harris, M. A. Klein, J. R. O'Dell, M. M. Hooper, J. D. Bradley, C. O. Bingham, M. H. Weisman, C. G. Jackson, N. E. Lane, J. J. Cush, L. W. Moreland, H. R. Schumacher Jr, C. V. Oddis, F. Wolfe, J. A. Molitor, D. E. Yocum, T. J. Schnitzer, D. E. Furst, A. D. Sawitzke, H. Shi, K. D. Brandt, R. W. Moskowitz and H. J. Williams, *N. Engl. J. Med.*, 2006, **354**, 795–808.

2 W. Pan, Y. Zhang, G. Liang, S. P. Vincent and P. Sinaÿ, *Chem. Commun.*, 2005, **27**, 3445–3447.

3 M. Irmak, A. Groschner and M. M. K. Boysen, *Chem. Commun.*, 2007, **2**, 177–179.

4 M. Veerapandian, S. Sadhasivam, J. Choi and K. Yun, *Chem. Eng. J.*, 2012, **209**, 558–567.

5 K. G. Thakur, D. Ganapathy and G. Sekar, *Chem. Commun.*, 2011, **47**, 5076–5078.

6 I. Szulc, R. Kołodziuk and A. Zawisza, *Tetrahedron*, 2018, **74**, 1476–1485.

7 E. M. Dangerfield, C. H. Plunkett, A. L. Win-Mason, B. L. Stocker and M. S. Timmer, *J. Org. Chem.*, 2010, **75**, 5470–5477.

8 K.-L. Chang, M. M. L. Zulueta, X.-A. Lu, Y.-Q. Zhong and S.-C. Hung, *J. Org. Chem.*, 2010, **75**, 7424–7427.

9 S.-J. Kim and H. Cho, *Bull. Korean Chem. Soc.*, 2015, **36**, 1916–1918.

10 M. Emmadi and S. S. Kulkarni, *Nat. Protoc.*, 2013, **8**, 1870–1889.

11 K. Skarbek and M. J. Milewska, *Carbohydr. Res.*, 2016, **434**, 44–71.

12 A. Gomm, E. O'Reilly and C. Opin, *Chem. Biol.*, 2018, **43**, 106–112.

13 F. Steffen-Munsberg, C. Vickers, H. Kohls, H. Land, H. Mallin, A. Nobili, L. Skalden, T. van den Bergh, H. J. Joosten, P. Berglund, M. Höhne and U. T. Bornscheuer, *Biotechnol. Adv.*, 2015, **33**, 566–604.

14 F. Subrizi, L. Benhamou, J. M. Ward, T. D. Sheppard and H. C. Hailes, *Angew. Chem., Int. Ed.*, 2019, **58**, 3854–3858.

15 R. Cairns, A. Gomm, J. Ryan, T. Clarke, E. Kulcinskaja, K. Butler and E. O'Reilly, *ACS Catal.*, 2019, **9**, 1220–1223.

16 V. Aumala, F. Mollerup, E. Jurak, F. Blume, J. Karppi, A. E. Koistinen, E. Schuiten, M. Voß, U. T. Bornscheuer, J. Deska and E. R. Master, *ChemSusChem*, 2019, **12**, 848–857.

17 C. Leitner, J. Volc and D. Haltrich, *Appl. Environ. Microbiol.*, 2001, **67**, 3636–3644.

18 M. Prongjit, J. Sucharitakul, T. Wongnate, D. Haltrich and P. Chaiyen, *Biochemistry*, 2009, **48**, 4170–4180.

19 W. Pitsawong, J. Sucharitakul, M. Prongjit, T.-C. Tan, O. Spadiut, D. Haltrich, C. Divne and P. Chaiyen, *J. Biol. Chem.*, 2010, **285**, 9697–9705.

20 T. Wongnate, P. Surawatanawong, S. Visitsatthawong, J. Sucharitakul, N. S. Scrutton and P. Chaiyen, *J. Am. Chem. Soc.*, 2014, **136**, 241–253.

21 S. Şahin, T. Wongnate, L. Chuaboon, P. Chaiyen and E. H. Yu, *Biosens. Bioelectron.*, 2018, **107**, 17–25.

22 L. Chuaboon, T. Wongnate, P. Punthong, C. Kiattisewee, N. Lawan, C. Y. Hsu, C. H. Lin, U. T. Bornscheuer and P. Chaiyen, *Angew. Chem., Int. Ed.*, 2019, **58**, 2428–2432.

23 T. Wongnate, P. Surawatanawong, L. Chuaboon, N. Lawan and P. Chaiyen, *Chem.–Eur. J.*, 2019, **25**, 4460–4471.

24 P. Punthong, S. Visitsatthawong, L. Chuaboon, P. Chaiyen and T. Wongnate, *Mol. Catal.*, 2022, **533**, 112753.

25 M. Thomsen, L. Skalden, G. J. Palm, M. Hohne, U. T. Bornscheuer and W. Hinrichs, *Acta Crystallogr., Sect. D:Biol. Crystallogr.*, 2014, **70**, 1086–1093.

26 M. S. Humble, K. E. Cassimjee, M. Håkansson, Y. R. Kimbung, B. Walse, V. Abedi, H.-J. Federsel, P. Berglund and D. T. Logan, *FEBS J.*, 2012, **279**, 779–792.

27 A. P. Green, N. J. Turner and E. O'Reilly, *Angew. Chem., Int. Ed.*, 2014, **53**, 10714–10717.

28 F. Steffen-Munsberg, C. Vickers, A. Thontowi, S. Schätzle, T. Tumlirsch, M. Svedendahl Humble, H. Land, P. Berglund, U. T. Bornscheuer and M. Höhne, *ChemCatChem*, 2013, **5**, 150–153.

29 M. Kollipara, P. Matzel, M. Sowa, S. Brott, U. T. Bornscheuer and M. Höhne, *Appl. Microbiol. Biotechnol.*, 2022, **106**, 5563–5574.

30 K. E. Cassimjee, B. Manta and F. Himo, *Org. Biomol. Chem.*, 2015, **13**, 8453–8464.

31 A. Jurcik, D. Bednar, J. Byska, S. M. Marques, K. Furmanova, L. Daniel, P. Kokkonen, J. Brezovsky, O. Strnad, J. Stourac, A. Pavelka, M. Manak, J. Damborsky and B. Kozlikova, *Bioinformatics*, 2018, **34**, 3586–3588.

32 J. Ø. Madsen and J. M. Woodley, *ChemCatChem*, 2023, **15**, e202300560.

33 B. M. Hallberg, C. Leitner, D. Haltrich and C. Divne, *J. Mol. Biol.*, 2004, **341**, 781–796.

34 T.-C. Tan, D. Haltrich and C. Divne, *J. Mol. Biol.*, 2011, **409**, 588–600.

35 A. D. Becke, *J. Chem. Phys.*, 1993, **98**, 5648–5652.

36 C. Lee, W. Yang and R. G. Parr, *Phys. Rev. B:Condens. Matter Mater. Phys.*, 1988, **37**, 785–789.

37 P. J. Stephens, F. J. Devlin, C. F. Chabalowski and M. J. Frisch, *J. Phys. Chem.*, 1994, **98**, 11623–11627.

38 P. C. Hariharan and J. A. Pople, *Theor. Chim. Acta*, 1973, **28**, 213–222.

39 G. A. Petersson and M. A. Al-Laham, *J. Chem. Phys.*, 1991, **94**, 6081–6090.

40 G. A. Petersson, A. Bennett, T. G. Tensfeldt, M. A. Al-Laham, W. A. Shirley and J. Mantzaris, *J. Chem. Phys.*, 1988, **89**, 2193–2218.

41 M. J. Frisch, G. W. Trucks, H. B. Schlegel, G. E. Scuseria, M. A. Robb, J. R. Cheeseman, G. Scalmani, V. Barone, G. A. Petersson, H. Nakatsuji, X. Li, M. Caricato, A. V. Marenich, J. Bloino, B. G. Janesko, R. Gomperts, B. Mennucci, H. P. Hratchian, J. V. Ortiz, A. F. Izmaylov, J. L. Sonnenberg, D. B. Williams-Young, F. Ding, F. Lipparini, F. Egidi, J. Goings, B. Peng, A. Petrone, T. Henderson, D. Ranasinghe, V. G. Zakrzewski, J. Gao, N. Rega, G. Zheng, W. Liang, M. Hada, M. Ehara,

K. Toyota, R. Fukuda, J. Hasegawa, M. Ishida, T. Nakajima, Y. Honda, O. Kitao, H. Nakai, T. Vreven, K. Throssell, J. A. Montgomery Jr, J. E. Peralta, F. Ogliaro, M. J. Bearpark, J. J. Heyd, E. N. Brothers, K. N. Kudin, V. N. Staroverov, T. A. Keith, R. Kobayashi, J. Normand, K. Raghavachari, A. P. Rendell, J. C. Burant, S. S. Iyengar, J. Tomasi, M. Cossi, J. M. Millam, M. Klene, C. Adamo, R. Cammi, J. W. Ochterski, R. L. Martin, K. Morokuma, O. Farkas, J. B. Foresman and D. J. Fox, *Gaussian 16 Rev. C.01*, Wallingford, CT, 2016.

42 G. M. Morris, R. Huey and A. J. Olson, *Curr. Protoc. Bioinf.*, 2008, **24**(8), 1–40.

43 M. F Sanner, *J. Mol. Graphics*, 1999, **17**, 57–61.

44 T. J. Dolinsky, J. E. Nielsen, J. A. McCammon and N. A. Baker, *Nucleic Acids Res.*, 2004, **32**, W665–W667.

45 R. W. W. Hooft, C. Sander and G. Vriend, *Proteins:Struct., Funct., Bioinf.*, 1996, **26**, 363–376.

46 O. Trott and A. J. Olson, *J. Comput. Chem.*, 2010, **31**, 455–461.